

Structural studies of L1₀ FePt nanoparticles

T. J. Klemmer,^{a)} N. Shukla, C. Liu, X. W. Wu, E. B. Svedberg, O. Mryasov,
R. W. Chantrell, and D. Weller
Seagate Research, Pittsburgh, Pennsylvania 15222

M. Tanase and D. E. Laughlin
Data Storage Systems Center, Carnegie Mellon University, Pittsburgh, Pennsylvania 15213

(Received 23 May 2002; accepted for publication 24 July 2002)

We have studied the lattice parameter changes of L1₀ FePt nanoparticles annealed to near equilibrium as a function of composition by x-ray diffraction. We have found that the (111) diffraction peak shifts linearly with composition, however, the *c* parameter mostly changes in the Pt rich compositions and the *a* parameter mostly changes in the Fe rich compositions with respect to the equiatomic composition. This causes the tetragonality of the L1₀ structure to be maximized near the Fe 50%/Pt 50% composition. The magnetic properties were measured at room temperature and at 5 K and are correlated to the structural changes occurring as a function of composition. © 2002 American Institute of Physics. [DOI: 10.1063/1.1507837]

Recently there has been much attention placed on the chemical synthesis of self assembled, monodispersed and chemically ordered L1₀ FePt nanoparticles for future ultra-high density magnetic storage.^{1,2} The ordered L1₀ phase of the FePt system is of particular interest because of the high magnetocrystalline anisotropy (MCA) ($\sim 6.6 \times 10^7$ ergs/cm³) that should allow the use of smaller particles but yet avoid thermal instabilities that give rise to superparamagnetic behavior.³

Although the magnetic properties of FePt nanoparticles have been studied as a function of composition,⁴ there is no known study in these nanoparticles of the lattice parameter changes that occur as the FePt composition is shifted away from the equiatomic composition. For bulk alloys these lattice parameters are known,⁵ however, for nanoparticle case the small size of the particles and the larger surface area could effect the crystalline structure and/or the ordering process. For the L1₀ phase there are two ways that the fcc cubic symmetry can be broken that will give rise to the high MCA. The first is the asymmetry of atomic sites produced by stacking of alternate planes of pure Fe and pure Pt along the *c* axis while along the *a* axis the planes have a mixture of Fe and Pt. As a consequence of the lower symmetry due to chemical ordering, structural changes of the unit cell also occur resulting in a difference of the lattice spacing perpendicular (*c* axis) and along (*a* axis) the same chemical species layers which is the second way of breaking the cubic symmetry. Of course these two effects are intimately related and their individual influence on MCA can only be modeled using first-principles theoretical methods.⁶ However, it is clear that the structural tetragonality of the L1₀ structure is an important property to monitor the degree of the chemical ordering and the correspondingly MCA of the crystal. For example, it is known that for bulk L1₀ alloys such as FePd and CoPt the highest magnetocrystalline anisotropy exists at the equiatomic composition which also coincides with the maximization of the tetragonality of the L1₀ phase.⁷ For magnetic

data storage this control of the magnetocrystalline anisotropy by varying the chemical composition is important in enabling the engineering of the write field coercivity of the media to the write field produced by the head. In this letter we report the structural changes that occur in chemically synthesized FePt L1₀ phase nanoparticle array as the composition changes from the equiatomic. We also use these measurements in the understanding of the magnetic properties of these nanoparticle arrays.

FePt nanoparticles roughly 4 nm [measured using transmission electron microscopy (TEM)] in diameter and coated with a 2 nm surfactant layer are prepared from Fe(CO)₅ and Pt(acac)₂ using a well known synthesis route.¹ The samples used for x-ray diffraction (XRD) are prepared by evaporating a solution of the FePt nanoparticles in hexane with excess surfactant on a SiO₂ coated Si wafer. XRD studies are carried out with a Philips X'PERT PRO MRD equipped with Cu K_α radiation and an x-ray mirror using primarily asymmetric glancing incidence scans with the incident angle set at 3°. Superconducting quantum interference device (SQUID) magnetometry was used to characterize the magnetic properties of the nanoparticles at RT and 5 K. The samples were heat treated with a rapid thermal anneal at a relatively high temperature of 650 °C for 30 min, in an atmosphere of Ar gas with less than 1 ppm of O₂.

Dai *et al.*⁸ have shown that with these high temperature anneals (>600 °C) a particle coalescence occurs which causes an increase of the particle size. This is also true in our samples. The focus of this letter, however, is to study the L1₀ ordering phase transformation driven to near equilibrium and the larger particle size (roughly 10 nm from TEM) aids to narrow the width of the XRD peaks. In Fig. 1(a) is plotted the composition of the nanoparticles measured by Rutherford backscattering spectrometry (RBS) as a function of the iron pentacarbonyl and platinum acetylacetonate ratio mixed during the synthesis (Fe/Pt ratio of the precursor). It is noticed that there is a loss of iron during the processing due to the low boiling point of iron pentacarbonyl. Figure 2 shows typical XRD scans for the samples used. All of the samples show

^{a)}Electronic mail: timothy.j.klemmer@seagate.com

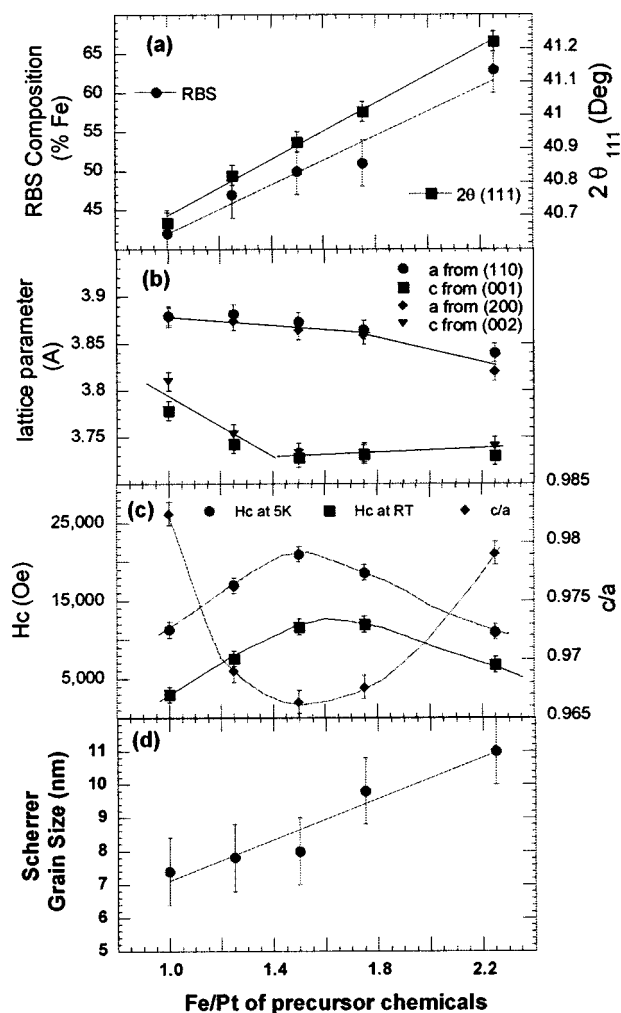


FIG. 1. (a) Chemical composition determined by RBS and 2θ values of the (111) peak; (b) lattice parameters calculated from the XRD superlattice reflections: (001) and (110) and the splitting of the fundamental (200)/(002); (c) coercivity and c/a ; and (d) Grain size measured from the (111) peak plotted against the Fe/Pt of the precursor chemicals.

the superlattice reflections (001) and (110) as well as some splitting of the (200)/(002) peak which signifies a tetragonality. Of interest is the fact that as more Fe is added to the system there is a noticeable shift of the (111) peak to higher angles. This shift can be used to monitor the relative composition of the FePt alloy. Also plotted in Fig. 1(a) is the (111) peak position that shows a linear behavior with the Fe/Pt ratio of the precursor. This shift in peak position is consistent with Vegard's Law⁹ that states that the lattice parameter of a binary solid solution is directly proportional to atomic per-

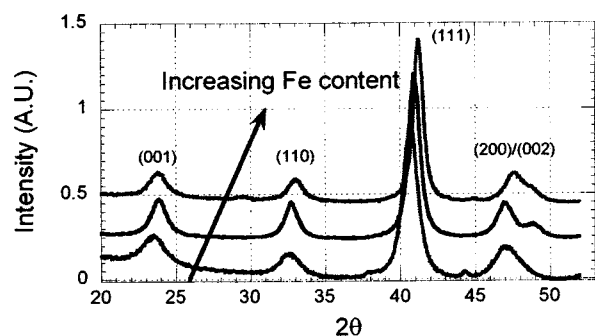


FIG. 2. XRD patterns for samples with different Fe/Pt compositions.

cent of the alloy. However, for the $L1_0$ structure the peak shift is more complicated because of its tetragonal structure.

In order to measure the lattice parameters (both c and a), the position of the superlattice peaks of (001) and (110) were determined by fitting and used to calculate the c parameter and a parameter, respectively. Additionally the (200)/(002) peak was deconvoluted and used to calculate the c and a lattice parameters. Figure 1(b) is a plot of these measurements as a function of the Fe/Pt of precursor. It should be noted that the Fe/Pt ratio of precursor equal to ~ 1.5 is where the RBS 50%Fe composition falls. With the addition of Pt it is noticed that there is very little change in the a parameter but the c parameter tends to get larger. This is not surprising because $FePt_3$ ($L1_2$ structure) is cubic with lattice parameter $a \sim 0.387$ nm which is near the a parameter for the $L1_0$ phase (~ 0.385 nm).¹⁰ It is expected that as the composition becomes Pt rich from the equiatomic $L1_0$ phase that the extra Pt must substitutionally sit on the $L1_0$ Fe sublattice which effectively will make the structure more like a cubic phase with the atomic positions in the vicinity of the defect similar to the $L1_2$ phase. Additionally, as the composition is pushed Fe rich from the 50% Fe region there seems to be a small change in the c parameter while the a parameter is changing faster and getting smaller. Again this is not surprising for the same reason as given earlier with the realization the $PtFe_3$ is cubic $L1_2$ with lattice parameter $a \sim 0.375$ nm which is near the c -axis parameter for $L1_0$ at ~ 0.371 nm.¹⁰ The lattice parameters measured here are in close agreement with those measured for bulk alloys of the same composition⁵ except for the low Fe content nanoparticles. The reason for this discrepancy seems to bring into question the bulk data where a 40% Fe alloy had an order parameter = 1 which is not possible for off stoichiometric ordered alloys. Another interesting observation in the data presented here is that the lattice parameters calculated from the superlattice reflections and the fundamental (200)/(002) splitting match very well. However, larger deviations are seen when the a parameter is changing quickly (high Fe content) and when the c parameter is changing quickly (high Pt content). We believe that this difference stems from the fact that the fundamental reflection is obtained from all the fcc based material (ordered and disordered) while the superlattice reflections are only obtained from the regions of the ordered material.

The relationship between the structural parameters of the $L1_0$ phase and the magnetics are summarized in Fig. 1(c). The c/a is plotted with the coercivities measured at room temperature and at 5 K. The tetragonality is found to be maximized (c/a is minimized) at the 50% Fe composition and is determined to be 0.966 which is similar to bulk powders of FePt.¹⁰ The room temperature coercivity has what may be a peak shifted slightly from the minimum of c/a while the 5 K coercivity has a maximum which fits very well with the minimum in c/a . We believe that this discrepancy is related to the actual microstructure of the films. Plotted in Fig. 1(d) is the grain size calculated by the Scherrer equation using the full width at half maximum of the (111) peak. It can be seen that the grain size clearly increases with increasing Fe content. It is not clear if this difference is from the actual nanoparticles being larger in the as-synthesized

sample or if there is a difference in the sintering phenomenon that gives larger particle size for the Fe rich alloy. However, it is clear that the larger particle size would cause a shift of the peak in the room temperature coercivity to Fe rich compositions (larger particles) because of the larger $K_u V$ term and therefore less thermally induced reduction of the coercivity due to superparamagnetic effects. Clearly the 5 K coercivity measurements minimize this microstructural/particle size issue and the peak coercivity coincides with the equiatomic composition.

The structural parameters of $L1_0$ FePt nanoparticles have been systematically studied as a function of composition. The small size of the nanoparticles does not seem to have a strong effect on the crystalline structure. It is found that these nanoparticles have a peak low temperature coercivity which is strongly related to the change of the lattice parameters of the $L1_0$ phase. This observation presents evidence that MCA is strongly (coupled) correlated with the c/a ratio and the peak anisotropy coincides with the maximum tetragonality. This correlation can be understood, similarly to the bulk $L1_0$ alloys, using the notion that chemical ordering is a driving force for the structural changes and maximum tetragonality reflects the highest degree of the layered chemi-

cal order. We also suggest that following the ordering process by measuring the room temperature coercivity can give erroneous results because of the thermally induced reduction of the coercivity for small particles. Therefore, the low temperature measurements are critical for the understanding of the magnetic properties relationship to the intrinsic structure of the $L1_0$ crystal structure.

¹S. Sun, C. B. Murray, D. Weller, L. Folks, and A. Moser, *Science* **287**, 1989 (2000).

²S. Sun, D. Weller, and C. Murray, in *The Physics of Ultra-High-Density Magnetic Recording*, edited by M. L. Plumer, J. v. Ek, and D. Weller (Springer, New York, 2001), pp. 249–276.

³A. Moser and D. Weller, in *The Physics of Ultra-High-Density Magnetic Recording*, edited by M. L. Plumer, J. v. Ek, and D. Weller (Springer, New York, 2001), pp. 145–173.

⁴S. Sun, E. E. Fullerton, D. Weller, and C. B. Murray, *IEEE Trans. Magn.* **37**, 1239 (2001).

⁵A. Z. Men'shikov, Y. A. Dorofeyev, V. A. Kazantsev, and S. K. Sidorov, *Fiz. Met. Metalloved.* **38**, 505 (1974).

⁶O. Mryasov (unpublished).

⁷V. V. Maykov, A. Y. Yermakov, G. V. Ivanov, V. I. Khrabov, and L. M. Magat, *Phys. Met. Metallogr.* **67**, 76 (1989).

⁸Z. R. Dai, S. Sun, and Z. L. Wang, *Nano Letters* **1**, 443 (2001).

⁹B. D. Cullity, *Elements of X-ray Diffraction*, 2nd ed. (Addison-Wesley, Reading, MA, 1978).

¹⁰JCPDS-International Centre for Diffraction Data, 1999.